International Journal of Nanomedicine

Dovepress

open access to scientific and medical research

Open Access Full Text Article

ORIGINAL RESEARCH

Transferrin-modified nanostructured lipid carriers as multifunctional nanomedicine for codelivery of DNA and doxorubicin

This article was published in the following Dove Press journal:
International Journal of Nanomedicine
25 August 2014
Number of times this article has been viewed

Yiqun Han[1,†]
Ying Zhang[2,†]
Danni Li[3]
Yuanyuan Chen[1]
Jiping Sun[1]
Fansheng Kong[4]

[1]Department of Respiratory Medicine, General Hospital of Ji'nan Command, PLA, [2]Center of Interventional Therapy, Ji'nan Infectious Disease Hospital, [3]Department of Internal Neurology, Ji'nan Central Hospital Affiliated to Shandong University, [4]Department of Hematology, General Hospital of Ji'nan Command, PLA, Ji'nan, People's Republic of China

[†]These two authors contributed equally to this work

Background: Nanostructured lipid carriers (NLC), composed of solid and liquid lipids, and surfactants are potentially good colloidal drug carriers. The aim of this study was to develop surface-modified NLC as multifunctional nanomedicine for codelivery of enhanced green fluorescence protein plasmid (pEGFP) and doxorubicin (DOX).

Methods: Two different nanocarriers: pEGFP- and DOX-loaded NLC, and solid lipid nanoparticles (SLN) were prepared. Transferrin-containing ligands were used for the surface coating of the vectors. Their average size, zeta potential, and drug encapsulation capacity were evaluated. In vitro transfection efficiency of the modified vectors was evaluated in human alveolar adenocarcinoma cell line (A549 cells), and in vivo transfection efficiency of the modified vectors was evaluated in a mouse bearing A549 cells model.

Results: Transferrin-modified DOX and pEGFP coencapsulated NLC (T-NLC) has a particle size of 198 nm and a +19 mV surface charge. The in vitro cell viabilities of the T-NLC formulations were over 80% compared with the control. T-NLC displayed remarkably greater gene transfection efficiency and enhanced antitumor activity than DOX- and pEGFP-coencapsulated SLN in vivo.

Conclusion: The results demonstrate that T-NLC noticeably enhanced antitumor activity through the combination of gene therapy with chemotherapy. Also coating of active transferrin improved the lung cancer cell-targeting of the carriers. In summary, the novel gene and drug delivery system offers a promising strategy for the treatment of lung cancer.

Keywords: multifunctional delivery system, active targeting, transferrin modification, solid lipid nanoparticles

Introduction

Lung cancer is the leading cause of cancer-related deaths worldwide.[1–3] Chemotherapy still plays an important role as primary and supportive care in treating lung cancer.[4,5] However, the development of multidrug resistance of cancer cells, as well as systemic toxic side effects resulting from nonspecific localization of anticancer drugs to nontumor areas are major obstacles to the success of chemotherapy in treating many cancers.[6–8] Therefore, novel treatment strategies for lung cancer are urgently needed.[9–11] A new treatment, codelivering more than one therapeutic agent in one delivery system, has recently been shown to be more effective than monotherapy, by providing potential synergistic effects of different treatment mechanisms.[12,13] Currently, the codelivery of nucleic acids and chemotherapeutics has been proposed to achieve the combined effect of gene therapy and chemotherapy.[14–16] So far, attempts have been made to simultaneously deliver genes and drugs into cancer cells, using polymeric nanoparticles,[17] liposomes,[18] micelles,[19] dendrimers,[20] and other vectors.[21,22]

Correspondence: Fansheng Kong
Department of Hematology, General Hospital of Ji'nan Command, PLA, 25 Shifan Road, Ji'nan, 250031, People's Republic of China
Tel +86 0531 5166 6114
Email kongfanshengphd@hotmail.com

Solid lipid nanoparticles (SLN) have been presented as an alternate carrier to emulsions, liposomes, and polymeric nanoparticles for the codelivery of drugs and genes.[23] They have advantages such as less toxicity, low immunogenicity, and being easily modified, and our previous studies mainly focused on the development of SLNs.[24,25] A problem related to SLN is low drug encapsulation and increased drug expulsion during storage because of the recrystallization process.[26] Nanostructured lipid carriers (NLC) have been developed to overcome the drawbacks associated with SLNs.[27] They are the second lifetime of lipid nanocarriers. Contrasted with SLNs, NLCs show a higher loading capability by blending a fluid lipid with the solid lipid; achievement of a higher element drug stacking; and a lower likelihood of drug expulsion during storage.[28,29]

The effectiveness of nanomedicine could be further improved by actively targeting tumors with ligands coated to the surface of nanoparticles – these could be taken through a receptor-mediated endocytic pathway.[30] The overexpression of transferrin (Tf) receptors on tumor cells makes them effective targets for site-specific delivery of antitumor drugs and genes into proliferating cells.[31] Therefore, Tf-modified liposomes,[32,33] nanoparticles,[34,35] and dendrimers[36,37] have been widely investigated in recent years. Polyethyleneglycol-phosphatidylethanolamine (PEG-PE) conjugates with various PEG lengths, and terminal-targeted moieties can provide extremely stable and actively targeted vectors, which spontaneously accumulate at specific sites.[38–41] In this study, Tf-containing PEG-PE ligands (Tf-PEG-PE) were applied for the modification of NLC.

Doxorubicin (DOX) is widely used as a single agent or in combination with other regimens for various kinds of solid tumors.[42–44] However, dose-limiting toxic side effects, such as cardiotoxicity, myelosuppression, mucositis, and alopecia, limit the clinical application of DOX, owing to its nonspecifc distribution to healthy normal tissues.[45,46] It is necessary to improve the anticancer activity and reduce the systemic toxicity of DOX with development of drug delivery systems.[47] In the present research, DOX was chosen as a model drug and used along with the reported gene, for combination therapy of cancer treatment.

In this paper, Tf-PEG-PE-modified drug and gene-loaded NLCs and SLN (T-NLC and T-SLN) were prepared and examined in a mouse bearing A549 cells model. This system was expected to achieve stable drug- and gene-loading capacity; be recognized Tf receptor over A549 cells and internalized via receptor-mediated endocytosis; and finally, achieve codelivery, with both drug and gene therapeutic effects.

Materials and methods

Lipids and chemicals

Maleimide-PEG_{2000}-COOH was purchased from Shanghai Yare Biotech Inc, (Shanghai, People's Republic of China). Human Tf (iron-free) and L-α-phosphatidylethanolamine (PE) were purchased from Sigma-Aldrich Corp (St Louis, MO, USA). Tf-PEG-PE was synthesized by our group. 3-[4,5-dimehyl-2-thiazolyl]-2,5-diphenyl-2H-tetrazolium bromide (MTT), DOX·HCl, stearic acid, dimethyldioctadecylammonium bromide (DDAB), soybean phosphatidylcholine, triethylamine (TEA), and Tween® 80 were purchased from Sigma-Aldrich. Precirol® ATO 5 was generously provided by Gattefossé (St Priest, France). Injectable soya lecithin was obtained from Shanghai Taiwei Pharmaceutical Co, Ltd., (Shanghai, People's Republic of China). Enhanced green fluorescence protein plasmid (pEGFP)-N1 was provided by Shandong University (Shandong, People's Republic of China). Quant-iT™ PicoGreen® double-stranded (ds) DNA quantitation reagent was obtained from Invitrogen by Life Technologies (Carlsbad, CA, USA). All other chemicals were of analytical grade or higher.

Animals and tumor cells

Male C57BL/6 mice (18–22 g weight) were purchased from the Medical Animal Test Center of Shandong Province (Shandong, People's Republic of China). All animal experiments complied with the requirements of the National Act on the Use of Experimental Animals (People's Republic of China).

A549 human lung adenocarcinoma cells were obtained from the American Type Culture Collection (Manassas, VA, USA). Cells were cultured in Roswell Park Memorial Institute (RPMI) 1640 medium (Sigma-Aldrich), supplemented with 20% fetal bovine serum (Thermo Fisher Scientific Inc, Waltham, MA, USA) and 1.2 mL/100 mL penicillin–streptomycin (Sigma-Aldrich). All experiments were performed on cells in the exponential growth phase.

Preparation of drug- and gene-loaded NLC

Preparation of lipid phase

DOX·HCl was stirred with TEA in dimethyl sulfoxide (DMSO) overnight to obtain the DOX base.[4] The lipid dispersion was composed of Precirol ATO-5, olive oil, and lipoid S100 at a ratio of 3:1:1 (w/w/w). Soybean lecithin and DOX base were dissolved in 10 mL of acetone and added to the lipid dispersion to form the lipid phase.

Preparation of aqueous phase

The aqueous dispersion was prepared by dissolving pEGFP-N1, Tween-80, and DDAB in 10 mL of water. This aqueous solution was then stirred and heated to 30°C.

Preparation of NLC

The lipid phase was rapidly injected into the stirred aqueous phase (800 rpm) at 30°C, and the resulting suspension was then continually stirred at 600 rpm and 30°C until complete evaporation of the organic solvent. Then the resulting solution was stirred, in an ice bath, for 1 hour to stabilize the DOX- and pEGFP-loaded NLC.

Preparation of drug- and gene-loaded SLN

DOX- and pEGFP-loaded SLN complexes were prepared as follows: DOX·HCl was stirred with TEA in DMSO overnight to obtain the DOX base.[23] Blank SLN was prepared following the solvent displacement method. For the organic phase preparation, stearic acid (50 mg), injectable soya lecithin (30 mg), and DOX base were dissolved in 10 mL of acetone. For the aqueous phase preparation, 0.5% DDAB was dissolved and stirred at 600 rpm, at room temperature (RT). The organic phase was added dropwise into the aqueous phase and stirred until complete evaporation of the organic solvent. The pellet was vortexed and resuspended in Milli-Q water, washed three times, filtered through a 0.45 μm membrane, and adjusted to pH 7.0, with sodium hydroxide.

pEGFP was mixed with DOX-loaded SLN by vortexing the particles with a 5 mg/mL solution of pEGFP for 30 seconds. This was followed by incubation of the mixture for 30 minutes at RT, to form DOX- and pEGFP-loaded SLN.

Preparation of T-NLC and T-SLN

Tf-PEG-PE ligands were dissolved in 10 mL of phosphate-buffered saline (PBS). Then the solution was added dropwise into 20 mL of the NLC and SLN complexes that were stirred at 400 rpm, at RT, leading to the immediate modification.[24] Subsequently, free-Tf-PEG-PE was removed from modified NLC and SLN by gel chromatography, using a Sephadex® G-50 column. The obtained complexes were resuspended in Milli-Q water and filtered through a membrane with 0.45 μm pore size, to obtain T-NLC and T-SLN.

During the modification progress, the ligands masked the charge of the carriers, cause the changes of the potentials. Excessive coating of ligands may cause the aggregation of the particles and cause increase of the particle size. To determine the suitable ratio (Tf-PEG-PE ligand to NLC and SLN [w/w]) of the modification, different weight ratios of ligand to the carriers (L-to-C) were prepared. Zeta potential and size of the modified vectors were measured. The total L-to-C weight ratio was optimized by measuring the change in zeta potential and size.

Physicochemical characterization

The surface morphologies of both T-NLC and T-SLN were examined by transmission electronic microscopy (TEM). The mean particle size (PS), polydispersity index, and zeta potential, of NLC, SLN, T-NLC, and T-SLN were analyzed by a Zetasizer (3,000 SH; Malvern Instruments Ltd., Malvern, UK). The average particle size was expressed as volume mean diameter.

Gene-loading capacity (GL) and drug-encapsulation efficiency (EE)

The GL of T-NLC and T-SLN was determined with PicoGreen® fluorometry assay, by measuring the fluorescence and comparing this with the supernatant from blank NLC and SLN.[23] GL was calculated according to the linear calibration curve of pEGFP, according to the equation:

$$GL\ (\%) = (\text{Total pEGFP} - \text{free-pEGFP}) \times (\text{Total pEGFP})^{-1} \times 100. \quad (1)$$

The EE of the T-NLC and T-SLN formulations was determined by a subtraction method. Briefly, 0.2 mL of the formulation solution was centrifuged through a filter (EMD Millipore, Billerica, MA, USA) with molecular weight cutoff of 3 kDa. Free-DOX could pass through the filter, but T-NLC and T-SLN could not pass through the filter.[26] The supernatant was filtered through a membrane with 0.45 μm pore size and then analyzed by high-performance liquid chromatography (HPLC) to measure the encapsulation percentage. EE was calculated using the following equation:

$$EE\ (\%) = \text{Concentration of (Total DOX} - \text{Free-DOX)} \times \text{Concentration of total DOX}^{-1} \times 100. \quad (2)$$

In vitro cytotoxicity study

A549 cells were used to investigate the cytotoxicity of T-NLC, T-SLN, and nonmodified NLC and SLN by in vitro MTT assay. Cells were seeded in 48-well plates at 1×10^5 cells/well, then incubated at 37°C in a humidified atmosphere with 5% CO_2 for 24 hours. All samples were performed at the DOX concentrations of 0.5, 1.0, 1.5, and 2.0 μg/mL. Culture medium was used

as a blank control. After 48 hours of incubation, MTT solution (5 mg/mL) was added to each well, and the cells were incubated for another 4 hours. Cellular viability was assessed according to the MTT manufacturer's procedures, and the absorbance (Abs), at 570 nm, was measured using a microplate reader (Model 680; Bio-Rad Laboratories, Hercules, CA, USA). Cells without the addition of MTT reagents were used, as a blank, to calibrate the spectrophotometer to zero absorbance. The relative cell viability was calculated as follows:

$$\text{Cell viability (\%)} = (\text{Abs}_{\text{sample}} - \text{Abs}_{\text{blank}}) \times (\text{Abs}_{\text{control}} - \text{Abs}_{\text{blank}})^{-1} \times 100. \quad (3)$$

The drug concentration causing 50% inhibition (IC_{50}) was calculated using the Statistical Package for the Social Sciences Version 17 software (SPSS Inc., Chicago, IL, USA).[48]

In vivo gene transfection analysis and antitumor effect

Lung tumor-bearing C57BL/6 mice were prepared as follows: mice were housed at a temperature of 25°C±2°C and a relative humidity of 70%±5% under natural light/dark conditions for 1 week before dosing. Then the mice were inoculated subcutaneously (SC) in the right armpit with A549 cells suspended in PBS for 24 hours. After that, mice were divided into seven groups (six mice per group). The T-NLC, T-SLN, NLC, SLN, naked pEGFP solution (300 μL per injection), free-DOX solution, and 0.9% sodium chloride solution (blank control) were prepared and then injected into the mice via the tail vein.

For in vivo gene delivery study, mice were sacrificed at 48 hours or 72 hours after injection, and the tumor tissue samples were taken out. The tumor tissues were homogenized by pressing the samples through a 30 μm cell mesh with the plunger of a 10 mL syringe. Erythrocyte lysis buffer was then added during homogenization, to lyse the red blood cells. The homogenates were washed three times with PBS containing 0.5% bovine serum albumin and then filtered. The cells were finally obtained after centrifugation (4°C, 100 g) for 5 minutes and were seeded into 24-well plates in 1 mL of Dulbecco's Modified Eagle's Medium with 10% fetal bovine serum. The cells were then observed using an inverted fluorescence microscope (Olympus ZX71; Olympus Corp, Tokyo, Japan) for visualization of the fluorescent cells, and the picture was captured. For quantitation, the cells were washed with 1 mL of PBS (100 g, 4°C, for 5 minutes) and were detached with trypsin/ethylenediaminetetraacetic acid (EDTA). The supernatant was discarded and resuspended with 300 μL of PBS and added into the flow cytometer to quantitate the amount of A549 cells that were successfully transfected.

For in vivo anticancer activity evaluation, after drug administration, tumor growth was determined by caliper measurement every 3 days. Tumor volume was calculated as follows:[44]

$$\text{Tumor volume (mm}^3\text{)} = (\text{length} \times \text{width}^2)/2. \quad (4)$$

The antitumor efficacy of each formulation was evaluated by tumor inhibition rate and was calculated using the following formula:[48]

$$\text{Tumor inhibition rate (\%)} = (W_{\text{control}} - W_{\text{sample}}) \times W_{\text{control}}^{-1} \times 100, \quad (5)$$

where W_{sample} and $W_{control}$ represent the mean tumor weight of the samples and control group, respectively.

Statistical analysis

Results were reported as mean ± standard deviation (SD). Statistical significance was analyzed using the Student's *t*-test, with the *P*-value less than 0.05 ($P<0.05$) indicating significance.

Results

Modification ratio determination

The suitable ratios of NLC and SLN modification were determined both by zeta potential and size changes. As illustrated in Figure 1A, the optimum ratio of NLC modification was obtained at 3:10; while SLN modification was suitable at the ratio of 1:5 (Figure 1B).

Characterization of T-NLC and T-SLN

The transmission electron micrograph (TEM) pictures of the T-SLN and T-NLC were shown in Figure 2. T-SLN and T-NLC had dark coats on the white spherical-shaped particles but were slightly different in appearance.

The PS, polydispersity index, zeta potential, GL, and EE of NLC, SLN, T-NLC, and T-SLN were characterized and summarized in Table 1. The size of T-NLC (198 nm) was smaller than T-SLN (246 nm), and the zeta potential of T-NLC (+19 mV) was lower than T-SLN (+26 mV).

In vitro cytotoxicity study

In vitro cytotoxicity of free-DOX, NLC, SLN, T-NLC, and T-SLN were evaluated by MTT in A549 cells, at different

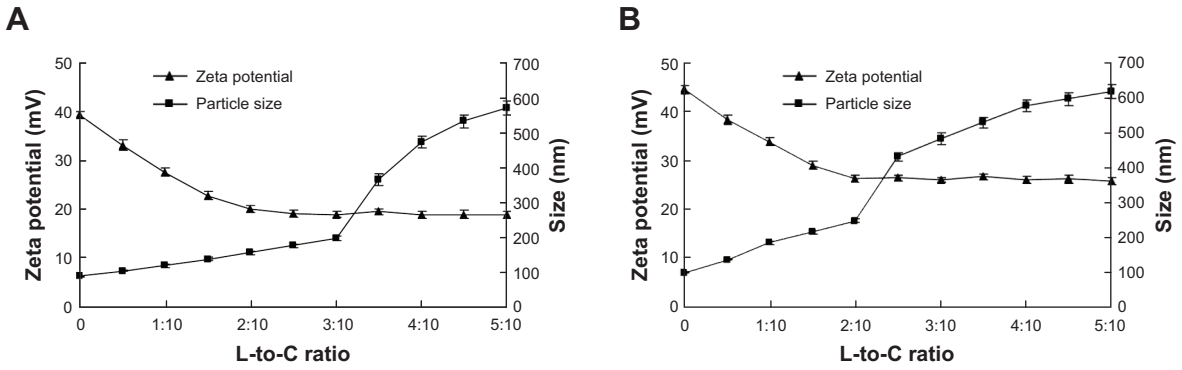

Figure 1 Suitable ratio determination results of (**A**) NLC modification and (**B**) SLN modification.
Notes: (**A**) The zeta potential of T-NLC decreased with the increase of L-to-C ratio, and was stable after the L-to-C ratio of 3:10. The size of the particles increased suddenly between 3:10 and 4:10. So the optimal ratio of NLC modification was 3:10. (**B**) The zeta potential of T-SLN decreased with the increase of L-to-C ratio, and was stable after the L-to-C ratio of 3:10. The size of the particles increased suddenly between 2:10 and 3:10. So the optimal ratio of SLN modification was 2:10.
Abbreviations: DOX, doxorubicin; L-to-C, ligand to carrier; NLC, nanostructured lipid carrier; pEGFP, enhanced green fluorescence protein plasmid; SLN, solid lipid nanoparticle; T-NLC, transferrin-modified DOX- and pEGFP-coencapsulated NLC; T-SLN, transferrin-modified DOX- and pEGFP-coencapsulated SLN.

concentrations. As illustrated in Figure 3, both free-DOX and different vectors inhibited the growth cells over the studied concentrations; as well, the cytotoxicity of all samples conformed to a concentration-dependent pattern. The cytotoxicity values of the NLC and SLN formulations were significantly higher than that of free-DOX solution at all concentrations. Moreover, T-NLC had the highest cytotoxic effect compared with T-SLN and nonmodified NLC ($P<0.05$). The IC_{50} values of free-DOX, NLC, SLN, T-NLC, and T-SLN were 1.88, 1.04, 1.36, 0.75, and 1.12 μg/mL respectively. The IC_{50} values for the nanocarrier samples were lower than free-DOX ($P<0.05$); T-NLC and T-SLN were lower than their nonmodified counterparts ($P<0.05$). The IC_{50} value of T-NLC was the lowest, accounting for the highest antitumor activity.

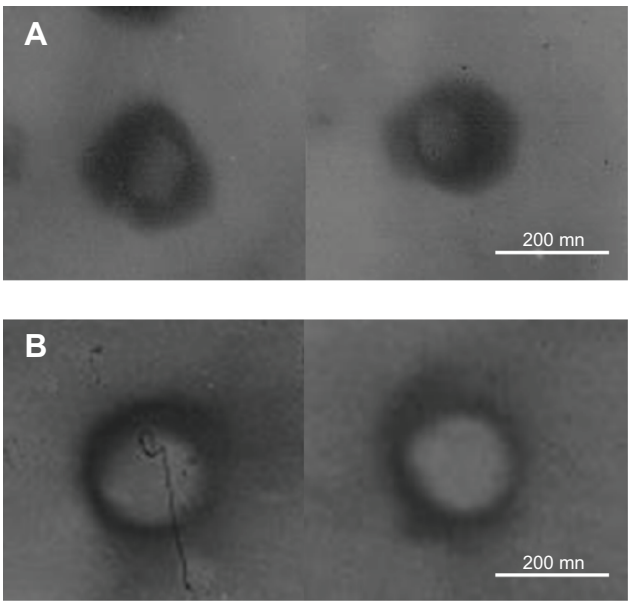

Figure 2 TEM imaging of T-SLN (**A**) and T-NLC (**B**).
Notes: Both T-SLN (**A**) and T-NLC (**B**) had dark coats on the white spherical shaped particles but were slightly different in appearance.
Abbreviations: DOX, doxorubicin; NLC, nanostructured lipid carrier; pEGFP, enhanced green fluorescence protein plasmid; SLN, solid lipid nanoparticle; T-NLC, transferrin-modified DOX- and pEGFP-coencapsulated NLC; T-SLN, transferrin-modified DOX- and pEGFP-coencapsulated SLN; TEM, transmission electron microscopy.

In vivo gene transfection analysis

The in vivo transfection efficiencies of naked pEGFP, SLN, NLC, T-SLN, and T-NLC were evaluated in tumor-bearing C57BL/6 mice at 48 hours and 72 hours of transfection. As illustrated in Figure 4, T-NLC showed higher transfection efficiency than other samples and showed good visualization of transfected green fluorescence cells.

Figure 5 shows the flow cytometry quantitation results of A549 cells that were successfully transfected by the vectors. T-NLC showed higher transfection efficiency than T-SLN and nonmodified NLC at 48 and 72 hours posttransfection ($P<0.05$). T-NLC and T-SLN showed higher transfection efficiency than their nonmodified counterparts ($P<0.05$).

In vivo anticancer therapy

The in vivo antitumor efficiency of the T-NLC, T-SLN, and NLC formulations were observed against A549 solid tumors in mice. The tumor growth curves of the T-NLC, T-SLN, NLC, SLN, free-DOX solution, and 0.9% sodium chloride solution groups are presented in Figure 6. Results indicate that tumor growth was significantly inhibited by the T-NLC, T-SLN, and NLC formulations ($P<0.05$). At 15 days of administration, tumor weight in mice treated with T-NLC, T-SLN, and NLC were inhibited by 66%, 39%, and 47% compared with control (Figure 7). T-NLC showed better

Table 1 PS, PI, ZP, GL, and EE of NLC, SLN, T-NLC, and T-SLN

Sample / Characteristic	NLC	SLN	T-NLC	T-SLN
PS (nm)	89.4±1.8	113.8±2.7	198.2±3.1	246.3±4.7
PI	0.12±0.02	0.14±0.03	0.13±0.02	0.15±0.04
ZP (mV)	+39.6±3.3	+44.7±3.9	+18.9±2.6	+26.1±3.8
GL (%)	91.3±2.7	93.1±1.8	92.2±1.6	91.4±2.1
EE (%)	88.3±2.2	81.9±2.9	86.7±2.7	80.6±3.9

Abbreviations: DOX, doxorubicin; EE, encapsulation efficiency; GL, gene-loading capacity; NLC, nanostructured lipid carrier; pEGFP, enhanced green fluorescence protein plasmid; PI, polydispersity index; PS, particle size; SLN, solid lipid nanoparticle; T-NLC, transferrin-modified DOX- and pEGFP-coencapsulated NLC; T-SLN, transferrin-modifed DOX- and pEGFP-coencapsulated SLN; ZP, zeta potential.

antitumor efficiency than nonmodified NLC. These results indicate that T-NLC and NLC had a greater antitumor effect than free-DOX and their SLN counterparts, in particular modified T-NLC.

Discussion

In previous studies, SLN were investigated for the delivery of genes,[24] drugs,[49] and for codelivery of both.[26] SLNs offered many advantages in the delivery of therapeutics and had impressive results in antitumor therapy. However, SLN formulations face the problems of low drug encapsulation and increased drug expulsion during storage.[50] In the present research, NLCs were developed to overcome the drawbacks of SLNs.

Firstly, drug- and gene-loaded NLC and SLN were prepared. Tf-PEG-PE ligands were synthesized as in our former report,[51] and T-NLC and T-SLN were prepared. During the synthesis, the positively charged terminal amino group of PE was conjugated with PEG via an amide linkage; thus, the negatively charged phosphate group was exposed and could readily absorb onto the cationic NLC/SLN surface by charge attraction.[52] Also, the PE end of the ligands could insert into the lipid surface of the carriers through lipophilic interaction.[51] During the modification progress, the ligands masked the surface charge of the carriers, causing the decrease of the zeta potential. On the other hand, no further change of the potential signaled the completion of modification. Ideally, the more ligands modifed onto the particles the better the targeting effect. However, excessive coating of ligands may cause the aggregation of the particles, leading to a sudden increase in particle size. Figure 1 shows the modification ratio determined by these two factors. The zeta potential of T-NLC was stable after the L-to-C ratio of 3:10 but suddenly increased between 3:10 and 4:10 (Figure 1A). The optimal ratio of NLC modification, then, is 3:10. The zeta potential of T-SLN was stable after the L-to-C ratio of 3:10 but increased suddenly between 2:10 and 3:10 (Figure 1B). So the optimal ratio of SLN modification has to be 2:10. These two ratios of T-NLC and T-SLN formulation were determined and used as the confirmed formula for the further studies.

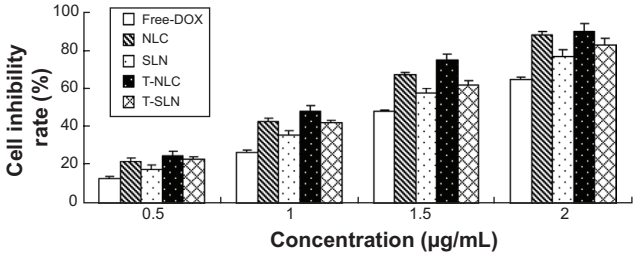

Figure 3 Cell inhibitory rate using different vectors by MTT assay.
Notes: All samples of different vectors were performed at the DOX concentrations of 0.5, 1.0, 1.5, and 2.0 μg/mL. Both free-DOX and different vectors inhibited the growth cells over the studied concentrations. The cytotoxicity values of the NLC formulations were significantly higher than that of free-DOX solution and SLN at all concentrations ($P<0.05$). T-NLC had the highest cytotoxic effect compared with other vectors ($P<0.05$).
Abbreviations: DOX, doxorubicin; MTT, 3-[4,5-dimethyl-2-thiazolyl]-2,5-diphenyl-2H-tetrazolium bromide; NLC, nanostructured lipid carrier; pEGFP, enhanced green fluorescence protein plasmid; SLN, solid lipid nanoparticle; T-NLC, transferrin-modified DOX- and pEGFP-coencapsulated NLC; T-SLN, transferrin-modified DOX- and pEGFP-coencapsulated SLN.

After formulation preparation, the physicochemical properties of different samples, including PS, polydispersity index, zeta potential, GL, and EE were characterized (Table 1). The size of T-NLC was 198 nm, smaller than T-SLN (246 nm). PS can influence the distribution of nanoparticles.[53] A smaller PS is an advantage for the vectors as this prolongs circulation time in the blood, decreases uptake by the liver, and improves bioavailability. Small particles can also minimal endocytosis, so destruction and clearance could be minimized. So T-NLC has superiority, with regard to PS, over T-SLN. The GL efficiencies of T-NLC and T-SLN were 92% and 91%, respectively. The data marked no significant difference from nonmodified NLC (91%) and SLN (93%). The results proved that the GL of all vectors are high (over 90%). The EEs of T-NLC, NLC, T-SLN, and SLN were 87%, 88%, 81%, and 82%. The results demonstrated that coating of Tf-PEG-PE

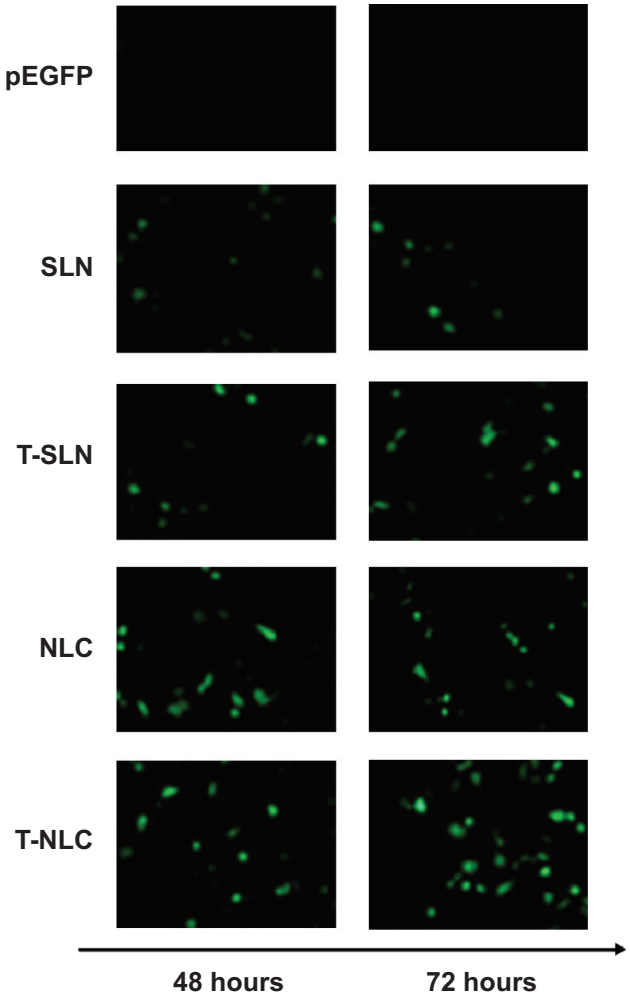

Figure 4 Fluorescent images of A549 cells transfected with different samples.
Notes: T-NLC samples got the best visual of transfected green fluorescence cells than other samples. NLC samples showed better visualization of transfected green fluorescence cells than their SLN counterparts.
Abbreviations: DOX, doxorubicin; NLC, nanostructured lipid carrier; pEGFP, enhanced green fluorescence protein plasmid; SLN, solid lipid nanoparticle; T-NLC, transferrin-modified DOX- and pEGFP-coencapsulated NLC; T-SLN, transferrin-modified DOX- and pEGFP-coencapsulated SLN.

ligands did not detach the gene and drug from the complexes and that the modified vectors were stable.

In vitro cytotoxicity of free-DOX, NLC, SLN, T-NLC, and T-SLN were evaluated (Figure 3). The cytotoxicity of all samples conformed to a concentration-dependent pattern. T-NLC had the highest cytotoxic effect compared with T-SLN and nonmodified NLC ($P<0.05$). The IC_{50} values of free-DOX, NLC, SLN, T-NLC, and T-SLN were 1.88, 1.04, 1.36, 0.75, 1.12 μg/mL, respectively. T-NLC and T-SLN were lower than their nonmodified counterparts ($P<0.05$). The IC_{50} value of T-NLC was the lowest. This could be explained by the positive charge on the particle surface having high electrostatic interaction with the negatively charged tumor surface, excellent compatibility of the NLC to the cell

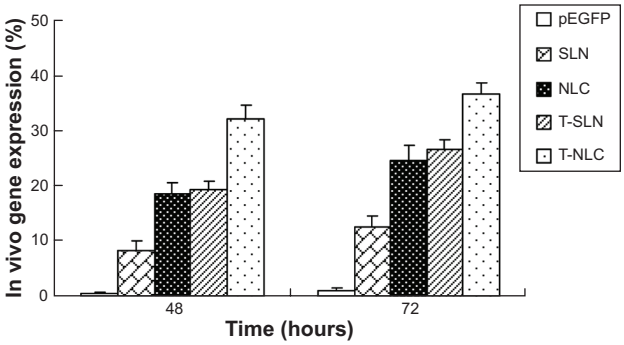

Figure 5 Flow cytometry results for the quantitation of different samples.
Notes: T-NLC showed higher transfection efficiency than T-SLN and nonmodified NLC at 48 and 72 hours posttransfection ($P<0.05$). T-NLC and T-SLN had higher transfection efficiency than their nonmodified counterparts ($P<0.05$).
Abbreviations: DOX, doxorubicin; NLC, nanostructured lipid carrier; pEGFP, enhanced green fluorescence protein plasmid; SLN, solid lipid nanoparticle; T-NLC, transferrin-modified DOX- and pEGFP-coencapsulated NLC; T-SLN, transferrin-modified DOX- and pEGFP-coencapsulated SLN.

membranes, and the targeting ability of the Tf ligands, which could mediate the intracellular gene and drug delivery via both endocytic and nonendocytic pathways.

The in vivo transfection efficiencies of naked pEGFP, SLN, NLC, T-SLN, and T-NLC were evaluated in tumor-bearing C57BL/6 mice. T-NLC showed higher transfection

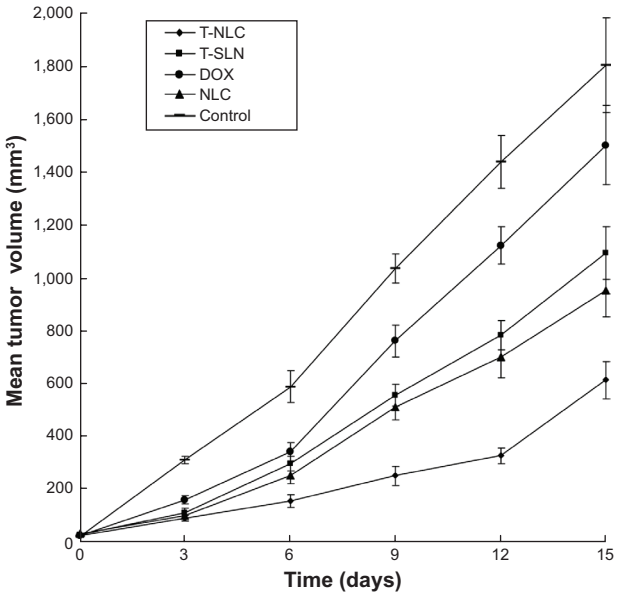

Figure 6 In vivo anticancer activity of different samples: the tumor growth curves of each group over the course of treatment.
Notes: Tumor growth was significantly inhibited by T-NLC, T-SLN, and NLC formulations at 3, 6, 9, 12, and 15 days of administration ($P<0.05$). At 15 days of administration, tumor volumes in mice treated with T-NLC, T-SLN, and NLC decreased compared with control ($P<0.05$). T-NLC showed better antitumor efficiency than nonmodified NLC and T-SLN ($P<0.05$).
Abbreviations: DOX, doxorubicin; NLC, nanostructured lipid carrier; pEGFP, enhanced green fluorescence protein plasmid; SLN, solid lipid nanoparticle; T-NLC, transferrin-modified DOX- and pEGFP-coencapsulated NLC; T-SLN, transferrin-modified DOX- and pEGFP-coencapsulated SLN.

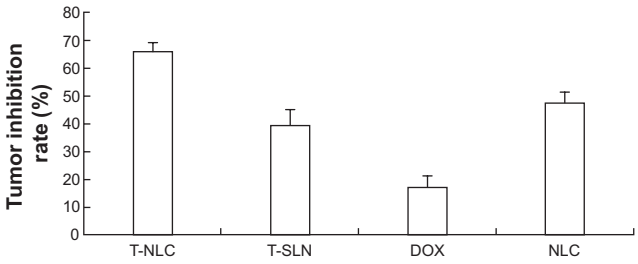

Figure 7 In vivo anticancer activity of different samples: calculated tumor inhibition rate after 15 days of treatment.
Notes: Tumor weight in mice treated with T-NLC, T-SLN, and NLC decreased by 66%, 39%, and 47% compared with control. Tumor weight in mice treated with T-NLC, T-SLN, and NLC decreased by 66%, 39%, and 47% compared with control, more than free-DOX formulation (decreased by 17%).
Abbreviations: DOX, doxorubicin; NLC, nanostructured lipid carrier; pEGFP, enhanced green fluorescence protein plasmid; SLN, solid lipid nanoparticle; T-NLC, transferrin-modified DOX- and pEGFP-coencapsulated NLC; T-SLN, transferrin-modified DOX- and pEGFP-coencapsulated SLN.

efficiency compared to other samples and showed good visualization of transfected green fluorescence cells (Figure 4) because pEGFP could express enhanced green fuorescence on the transfected cells. The flow cytometry quantitation results of the A549 cells are presented in Figure 5. T-NLC showed higher transfection efficiency than T-SLN and nonmodified NLC at 48 and 72 hours posttransfection ($P<0.05$). T-NLC and T-SLN both had higher transfection efficiency than their nonmodified counterparts ($P<0.05$). These results could be evidence of the Tf-mediated active targeting capability of T-NLC and T-SLN. This could also prove the better gene delivery ability of NLC formulations over SLN formulations.

The in vivo antitumor efficiency of the T-NLC, T-SLN, and NLC formulations were observed against A549 solid tumors in mice (Figure 6). Results indicate that tumor growth was significantly inhibited by the T-NLC, T-SLN, and NLC formulations ($P<0.05$). At 15 days of administration, tumor weight in the mice treated with T-NLC, T-SLN, and NLC decreased compared with control (Figure 7). T-NLC showed better antitumor efficiency than nonmodified NLC. These results indicate that T-NLC and NLC had a greater antitumor effect than free-DOX and their SLN counterparts, in particular modified T-NLC. The results regarding the in vivo gene and drug delivery efficiency of T-SLN were very impressive, showing that this could be a promising system for the codelivery of drugs and genes for the treatment of cancer. We believe these kinds of nanocarriers could be applied for the loading of drugs and/or genes for different types of tumor therapy.

Conclusion

In the current study, we illustrated that Tf-modified coencapsulated pEGFP- and DOX-loaded NLC were outstanding vehicles for tumor-targeted therapy. The results showed that, compared with the SLN formulation and their nonmodified counterparts, T-NLC can significantly improve the gene transfection efficiency of the vector and successfully control the tumor growth rate on tumor-bearing mice. In conclusion, with the modification of Tf, the modified codelivery system could improve the efficacy of cancer treatment and active-targeted gene delivery. These kinds of NLC systems should be used as excellent nanomedicine for the delivery of genes and/or drugs, leading to the increased efficiency of antitumor therapy.

Acknowledgments

The authors gratefully acknowledge Diah Mehera, MS (Publishing Program), New York University, and Ms Gabrielle Dugas, MS (Chemistry), Brandeis University, for language editing.

Disclosure

The authors report no conflicts of interest in this work.

References

1. Shepherd FA, Bunn PA, Paz-Ares L. Lung cancer in 2013: state of the art therapy for metastatic disease. *Am Soc Clin Oncol Educ Book*. 2013:339–346.
2. Sundaram S, Trivedi R, Durairaj C, Ramesh R, Ambati BK, Kompella UB. Targeted drug and gene delivery systems for lung cancer therapy. *Clin Cancer Res*. 2009;15(23):7299–7308.
3. Siegel R, Ward E, Brawley O, Jemal A. Cancer statistics, 2011: the impact of eliminating socioeconomic and racial disparities on premature cancer deaths. *CA Cancer J Clin*. 2011;61(4):212–236.
4. Taratula O, Kuzmov A, Shah M, Garbuzenko OB, Minko T. Nanostructured lipid carriers as multifunctional nanomedicine platform for pulmonary co-delivery of anticancer drugs and siRNA. *J Control Release*. 2013;171(3):349–357.
5. Carbone DP, Felip E. Adjuvant therapy in non-small cell lung cancer: future treatment prospects and paradigms. *Clin Lung Cancer*. 2011;12(5):261–271.
6. Bajelan E, Haeri A, Vali AM, Ostad SN, Dadashzadeh S. Co-delivery of doxorubicin and PSC 833 (Valspodar) by stealth nanoliposomes for efficient overcoming of multidrug resistance. *J Pharm Pharm Sci*. 2012;15(4):568–582.
7. Brannon-Peppas L, Blanchette JO. Nanoparticle and targeted systems for cancer therapy. *Adv Drug Deliv Rev*. 2004;56(11):1649–1659.
8. Gottesman MM, Fojo T, Bates SE. Multidrug resistance in cancer: role of ATP-dependent transporters. *Nat Rev Cancer*. 2002;2(1):48–58.
9. Kawabata A, Baoum A, Ohta N, et al. Intratracheal administration of a nanoparticle-based therapy with the angiotensin II type 2 receptor gene attenuates lung cancer growth. *Cancer Res*. 2012;72(8):2057–2067.
10. Othman N, In LL, Harikrishna JA, Hasima N. Bcl-xL silencing induces alterations in hsa-miR-608 expression and subsequent cell death in A549 and SK-LU1 human lung adenocarcinoma cells. *PLoS One*. 2013;8(12):e81735.
11. Shien K, Tanaka N, Watanabe M, et al. Anti-cancer effects of REIC/Dkk-3-encoding adenoviral vector for the treatment of non-small cell lung cancer. *PLoS One*. 2014;9(2):e87900.
12. Liu C, Liu F, Feng L, Li M, Zhang J, Zhang N. The targeted co-delivery of DNA and doxorubicin to tumor cells via multifunctional PEI-PEG based nanoparticles. *Biomaterials*. 2013;34(10):2547–2564.

13. Werner ME, Karve S, Sukumar R, et al. Folate-targeted nanoparticle delivery of chemo- and radiotherapeutics for the treatment of ovarian cancer peritoneal metastasis. *Biomaterials*. 2011;32(33):8548–8554.
14. Zheng C, Zheng M, Gong P, et al. Polypeptide cationic micelles mediated co-delivery of docetaxel and siRNA for synergistic tumor therapy. *Biomaterials*. 2013;34(13):3431–3438.
15. Loh XJ, Ong SJ, Tung YT, Choo HT. Co-delivery of drug and DNA from cationic dual-responsive micelles derived from poly(DMAEMA-co-PPGMA). *Mater Sci Eng C Mater Biol Appl*. 2013;33(8):4545–4550.
16. Zhao J, Mi Y, Feng SS. Targeted co-delivery of docetaxel and siPlk1 by herceptin-conjugated vitamin E TPGS based immunomicelles. *Biomaterials*. 2013;34(13):3411–3421.
17. Qiu B, Ji M, Song X, et al. Co-delivery of docetaxel and endostatin by a biodegradable nanoparticle for the synergistic treatment of cervical cancer. *Nanoscale Res Lett*. 2012;7(1):666.
18. Shim G, Han SE, Yu YH, et al. Trilysinoyl oleylamide-based cationic liposomes for systemic co-delivery of siRNA and an anticancer drug. *J Control Release*. 2011;155(1):60–66.
19. Nam K, Nam HY, Kim PH, Kim SW. Paclitaxel-conjugated PEG and arginine-grafted bioreducible poly (disulfide amine) micelles for co-delivery of drug and gene. *Biomaterials*. 2012;33(32):8122–8130.
20. Kaneshiro TL, Lu ZR. Targeted intracellular codelivery of chemotherapeutics and nucleic acid with a well-defined dendrimer-based nanoglobular carrier. *Biomaterials*. 2009;30(29):5660–5666.
21. Huang Y, Yu F, Park YS, et al. Co-administration of protein drugs with gold nanoparticles to enable percutaneous delivery. *Biomaterials*. 2010;31(34):9086–9091.
22. Chen AM, Zhang M, Wei D, et al. Co-delivery of doxorubicin and Bcl-2 siRNA by mesoporous silica nanoparticles enhances the efficacy of chemotherapy in multidrug-resistant cancer cells. *Small*. 2009;5(23):2673–2677.
23. Yu YH, Kim E, Park DE, et al. Cationic solid lipid nanoparticles for co-delivery of paclitaxel and siRNA. *Eur J Pharm Biopharm*. 2012;80(2):268–273.
24. Jiang Z, Sun C, Yin Z, et al. Comparison of two kinds of nanomedicine for targeted gene therapy: premodified or postmodified gene delivery systems. *Int J Nanomedicine*. 2012;7:2019–2031.
25. Wang W, Zhou F, Ge L, Liu X, Kong F. Transferrin-PEG-PE modified dexamethasone conjugated cationic lipid carrier mediated gene delivery system for tumor-targeted transfection. *Int J Nanomedicine*. 2012;7:2513–2522.
26. Han Y, Zhang P, Chen Y, Sun J, Kong F. Co-delivery of plasmid DNA and doxorubicin by solid lipid nanoparticles for lung cancer therapy. *Int J Mol Med*. 2014;34(1):191–196.
27. Selvamuthukumar S, Velmurugan R. Nanostructured lipid carriers: a potential drug carrier for cancer chemotherapy. *Lipids Health Dis*. 2012;11:159.
28. Müller RH, Radtke M, Wissing SA. Solid lipid nanoparticles (SLN) and nanostructured lipid carriers (NLC) in cosmetic and dermatological preparations. *Adv Drug Deliv Rev*. 2002;54(Suppl 1):S131–S155.
29. Saupe A, Wissing SA, Lenk A, Schmidt C, Müller RH. Solid lipid nanoparticles (SLN) and nanostructured lipid carriers (NLC) – structural investigations on two different carrier systems. *Biomed Mater Eng*. 2005;15(5):393–402.
30. Hong M, Zhu S, Jiang Y, et al. Novel anti-tumor strategy: PEG-hydroxycamptothecin conjugate loaded transferrin-PEG-nanoparticles. *J Control Release*. 2010;141(1):22–29.
31. Maruyama K, Ishida O, Kasaoka S, et al. Intracellular targeting of sodium mercaptoundecahydrododecaborate (BSH) to solid tumors by transferrin-PEG liposomes, for boron neutron-capture therapy (BNCT). *J Control Release*. 2004;98(2):195–207.
32. Gao JQ, Lv Q, Li LM, et al. Glioma targeting and blood–brain barrier penetration by dual-targeting doxorubincin liposomes. *Biomaterials*. 2013;34(22):5628–5639.
33. Salvati E, Re F, Sesana S, et al. Liposomes functionalized to overcome the blood–brain barrier and to target amyloid-β peptide: the chemical design affects the permeability across an in vitro model. *Int J Nanomedicine*. 2013;8:1749–1758.
34. Chiu RY, Tsuji T, Wang SJ, Wang J, Liu CT, Kamei DT. Improving the systemic drug delivery efficacy of nanoparticles using a transferrin variant for targeting. *J Control Release*. 2014;180:33–41.
35. Balasubramanian S, Girija AR, Nagaoka Y, et al. Curcumin and 5-fluorouracil-loaded, folate- and transferrin-decorated polymeric magnetic nanoformulation: a synergistic cancer therapeutic approach, accelerated by magnetic hyperthermia. *Int J Nanomedicine*. 2014;9:437–459.
36. Li Y, He H, Jia X, Lu WL, Lou J, Wei Y. A dual-targeting nanocarrier based on poly(amidoamine) dendrimers conjugated with transferrin and tamoxifen for treating brain gliomas. *Biomaterials*. 2012;33(15):3899–3908.
37. Koppu S, Oh YJ, Edrada-Ebel R, et al. Tumor regression after systemic administration of a novel tumor-targeted gene delivery system carrying a therapeutic plasmid DNA. *J Control Release*. 2010;143(2):215–221.
38. Koren E, Apte A, Sawant RR, Grunwald J, Torchilin VP. Cell-penetrating TAT peptide in drug delivery systems: proteolytic stability requirements. *Drug Deliv*. 2011;18(5):377–384.
39. Perche F, Patel NR, Torchilin VP. Accumulation and toxicity of antibody-targeted doxorubicin-loaded PEG-PE micelles in ovarian cancer cell spheroid model. *J Control Release*. 2012;164(1):95–102.
40. Sawant RR, Sriraman SK, Navarro G, Biswas S, Dalvi RA, Torchilin VP. Polyethyleneimine-lipid conjugate-based pH-sensitive micellar carrier for gene delivery. *Biomaterials*. 2012;33(15):3942–3951.
41. Biswas S, Dodwadkar NS, Sawant RR, Torchilin VP. Development of the novel PEG-PE-based polymer for the reversible attachment of specific ligands to liposomes: synthesis and in vitro characterization. *Bioconjug Chem*. 2011;22(10):2005–2013.
42. Gao X, Wang B, Wei X, et al. Preparation, characterization and application of star-shaped PCL/PEG micelles for the delivery of doxorubicin in the treatment of colon cancer. *Int J Nanomedicine*. 2013;8:971–982.
43. Yousefpour P, Atyabi F, Farahani EV, Sakhtianchi R, Dinarvand R. Polyanionic carbohydrate doxorubicin-dextran nanocomplex as a delivery system for anticancer drugs: in vitro analysis and evaluations. *Int J Nanomedicine*. 2011;6:1487–1496.
44. Jia Y, Yuan M, Yuan H, et al. Co-encapsulation of magnetic Fe_3O_4 nanoparticles and doxorubicin into biodegradable PLGA nanocarriers for intratumoral drug delivery. *Int J Nanomedicine*. 2012;7:1697–1708.
45. Hershman DL, McBride RB, Eisenberger A, Tsai WY, Grann VR, Jacobson JS. Doxorubicin, cardiac risk factors, and cardiac toxicity in elderly patients with diffuse B-cell non-Hodgkin's lymphoma. *J Clin Oncol*. 2008;26(19):3159–3165.
46. Kang YM, Kim GH, Kim JI, et al. In vivo efficacy of an intratumorally injected in situ-forming doxorubicin/poly(ethylene glycol)-b-polycaprolactone diblock copolymer. *Biomaterials*. 2011;32(20):4556–4564.
47. Lee CC, Gillies ER, Fox ME, et al. A single dose of doxorubicin-functionalized bow-tie dendrimer cures mice bearing C-26 colon carcinomas. *Proc Natl Acad Sci U S A*. 2006;103(45):16649–16654.
48. Yuan L, Liu C, Chen Y, Zhang Z, Zhou L, Qu D. Antitumor activity of tripterine via cell-penetrating peptide-coated nanostructured lipid carriers in a prostate cancer model. *Int J Nanomedicine*. 2013;8:4339–4350.
49. Wang W, Zhou F, Ge L, Liu X, Kong F. A promising targeted gene delivery system: folate-modified dexamethasone-conjugated solid lipid nanoparticles. *Pharm Biol*. 2014;52(8):1039–1044.
50. Jenning V, Gohla SH. Encapsulation of retinoids in solid lipid nanoparticles (SLN). *J Microencapsul*. 2001;18(2):149–158.
51. Kong F, Zhou F, Ge L, Liu X, Wang Y. Mannosylated liposomes for targeted gene delivery. *Int J Nanomedicine*. 2012;7:1079–1089.
52. Yu W, Liu C, Liu Y, Zhang N, Xu W. Mannan-modified solid lipid nanoparticles for targeted gene delivery to alveolar macrophages. *Pharm Res*. 2010;27(8):1584–1596.
53. Rahman HS, Rasedee A, How CW, et al. Zerumbone-loaded nanostructured lipid carriers: preparation, characterization, and antileukemic effect. *Int J Nanomedicine*. 2013;8:2769–2781.